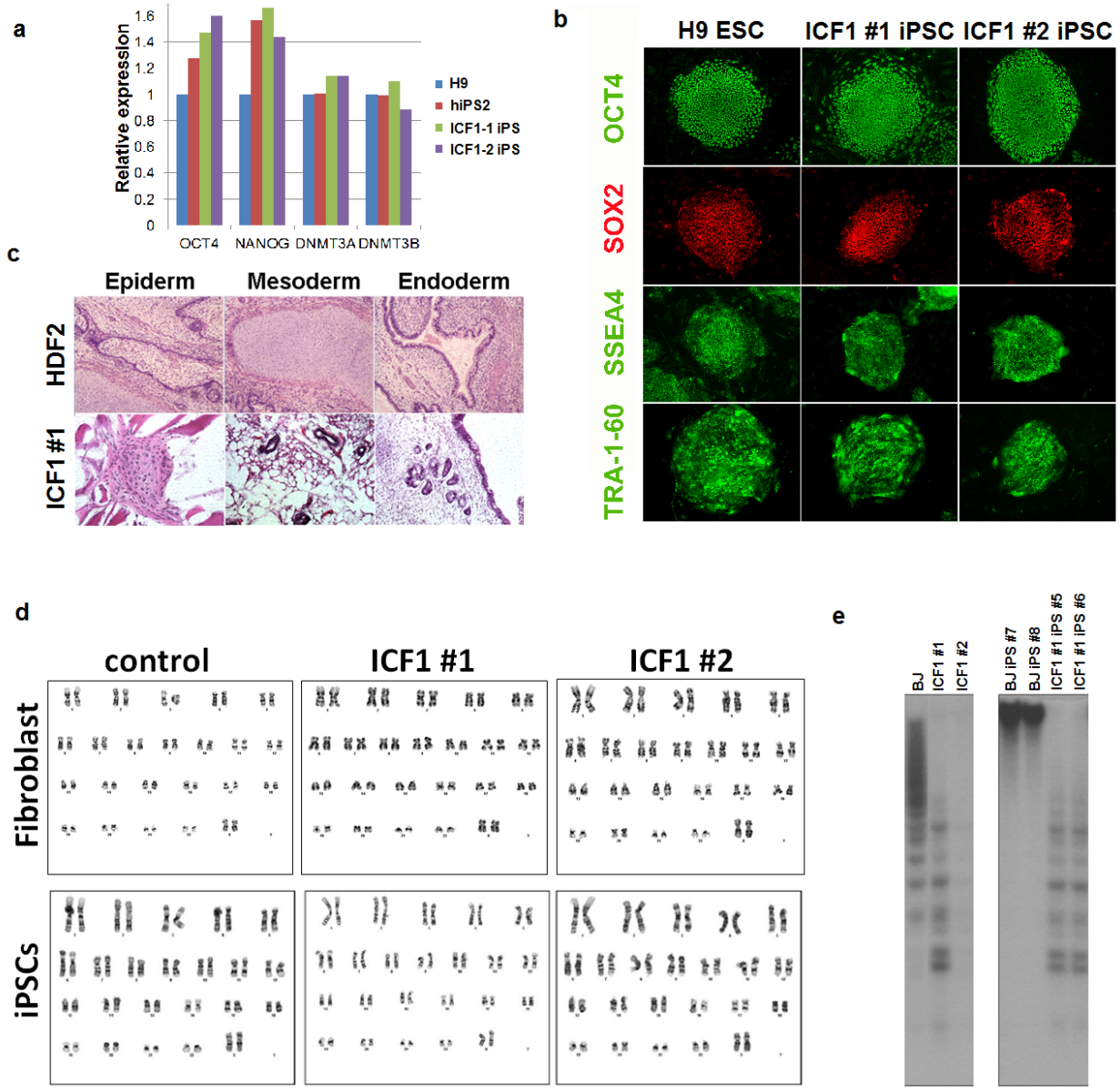

Figure S1. ICF iPSCs show normal pluripotency phenotypes. **A.** qRT-PCR on pluripotency genes shows equivalent expression levels between ICF iPSCs and normal iPSCs or hESCs. **B.** Immunostaining of pluripotency markers in reprogrammed ICF1 fibroblast cells. **C.** Histology sections of teratoma formations derived from ICF1-1 and control iPSCs. **D.** Karyotype of control and ICF1 fibroblasts and iPSCs. **E.** Southern blot for methylation status of human Satellite 2 repeats.

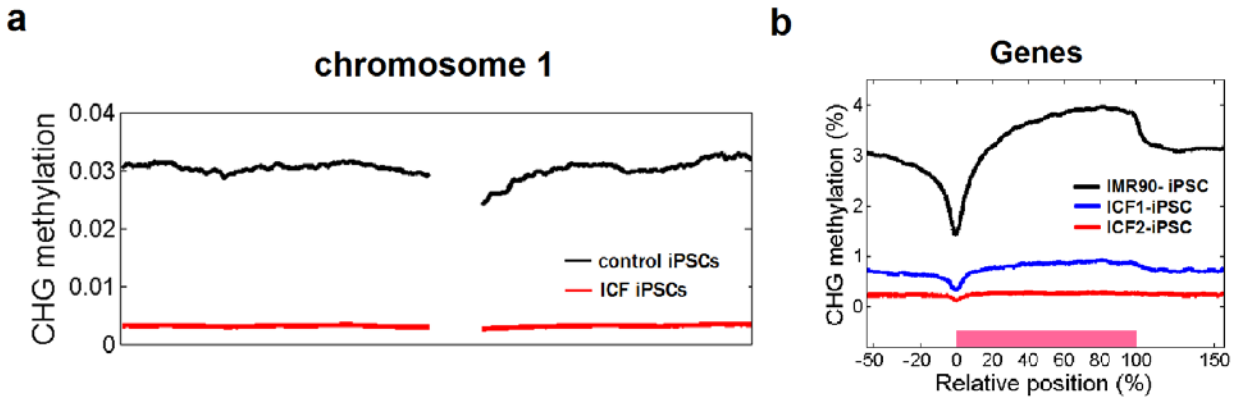

Figure S2. Non-CG patterns across (a) chromosomes and (b) genes. A. Chromosome view of average CHG methylation in control and ICF1 iPSCs. **B.** Metaplot of average CHG methylation profile across gene bodies in control and ICF1 iPSCs. CHH profiles are nearly identical to CHG profiles.

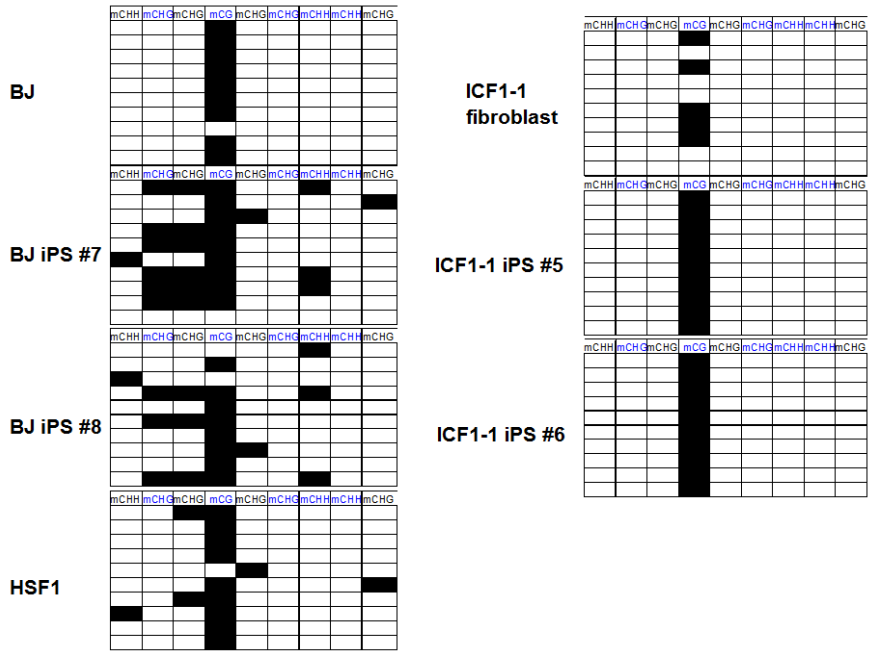

Figure S3. Conventional bisulfite sequencing validation. Bisulfite confirms dramatic differences in non-CG methylation between somatic and pluripotent stem cells (left column), and loss of non-CG methylation in ICF1-iPSCs (right column). PCR regions are exactly based on primers previously designed by Lister et al., 2009. BJ is a line of primary foreskin fibroblast.

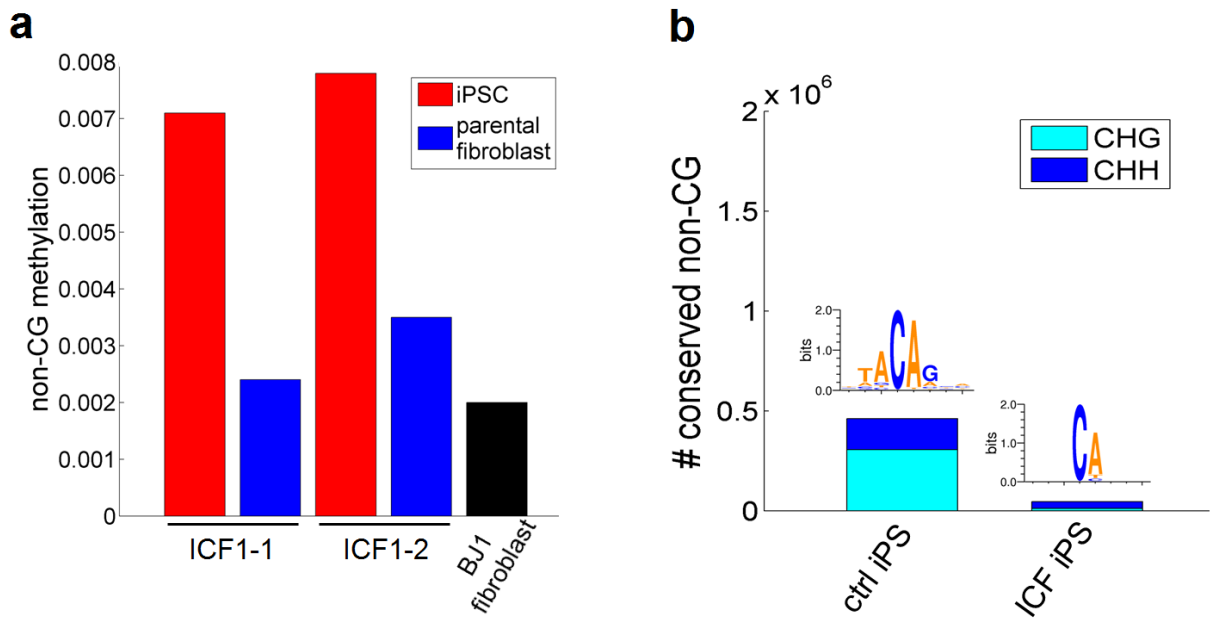

Figure S4. Residual non-CG methylation in ICF1 iPSCs. A) Bar plot showing levels of non-CG methylation in iPSCs and parental fibroblasts. As additional control, BJ1 fibroblasts are used to show non-CG methylation in normal fibroblast cells. All methylation levels in fibroblasts were measured via reduced representation bisulfite sequencing (RRBS).

B) Highly methylated non-CG sites (>0.3) shared between either control (IMR90 iPS and FF1911 iPS) or ICF1 (-1 and -2) cell lines are numerated in the bar plot. Sequence motif of conserved non-CGs are shown above the bar plot. Motif logo was generated by via http://weblogo.berkeley.edu/logo.cgi.

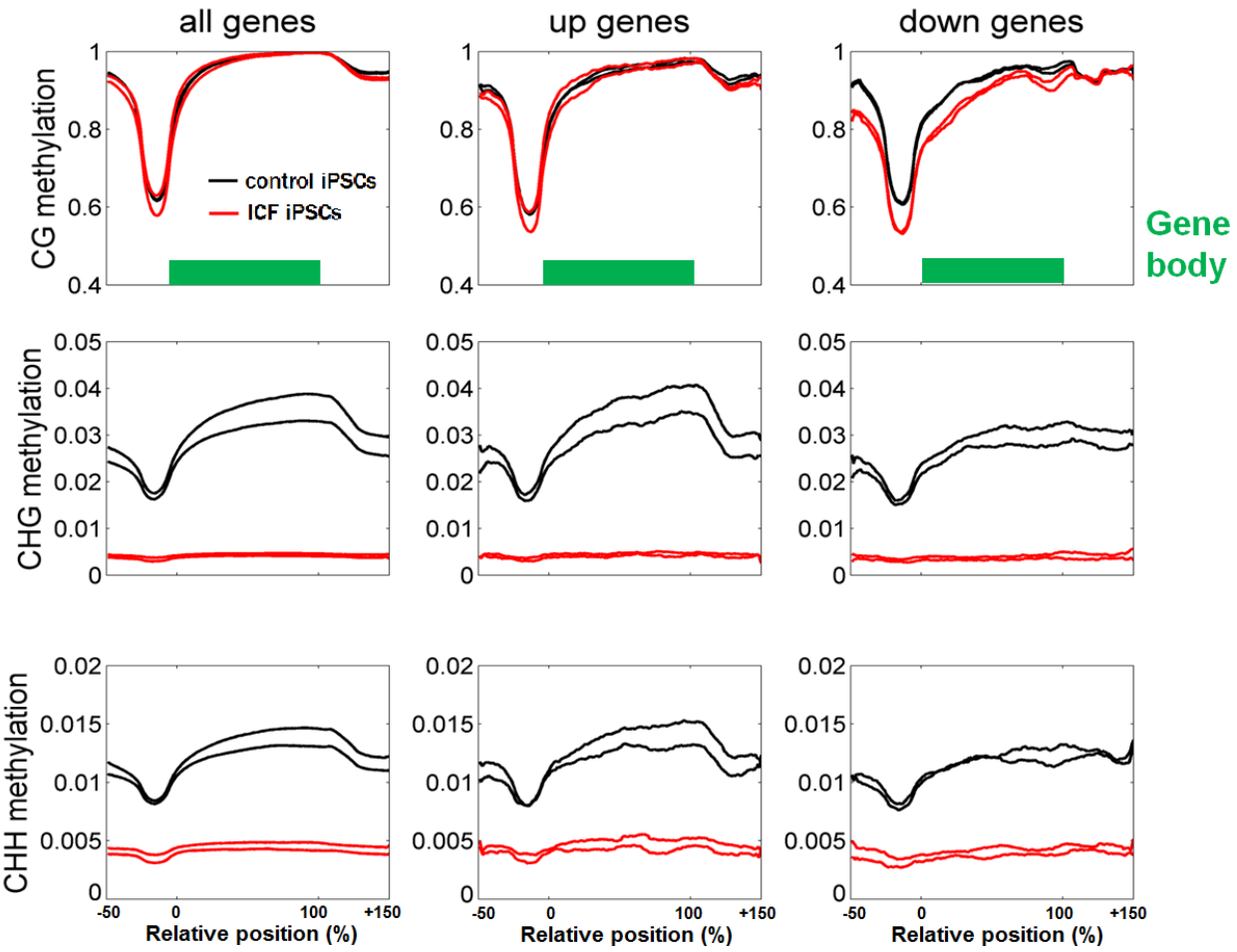

Figure S5. CG and non-CG methylation profile across gene bodies. Metaplots of average CG, CHG, and CHH methylation profile across gene bodies in control (IMR90iPSC, FF19.11iPSC) and ICF1 (-1 and -2) iPSCs.

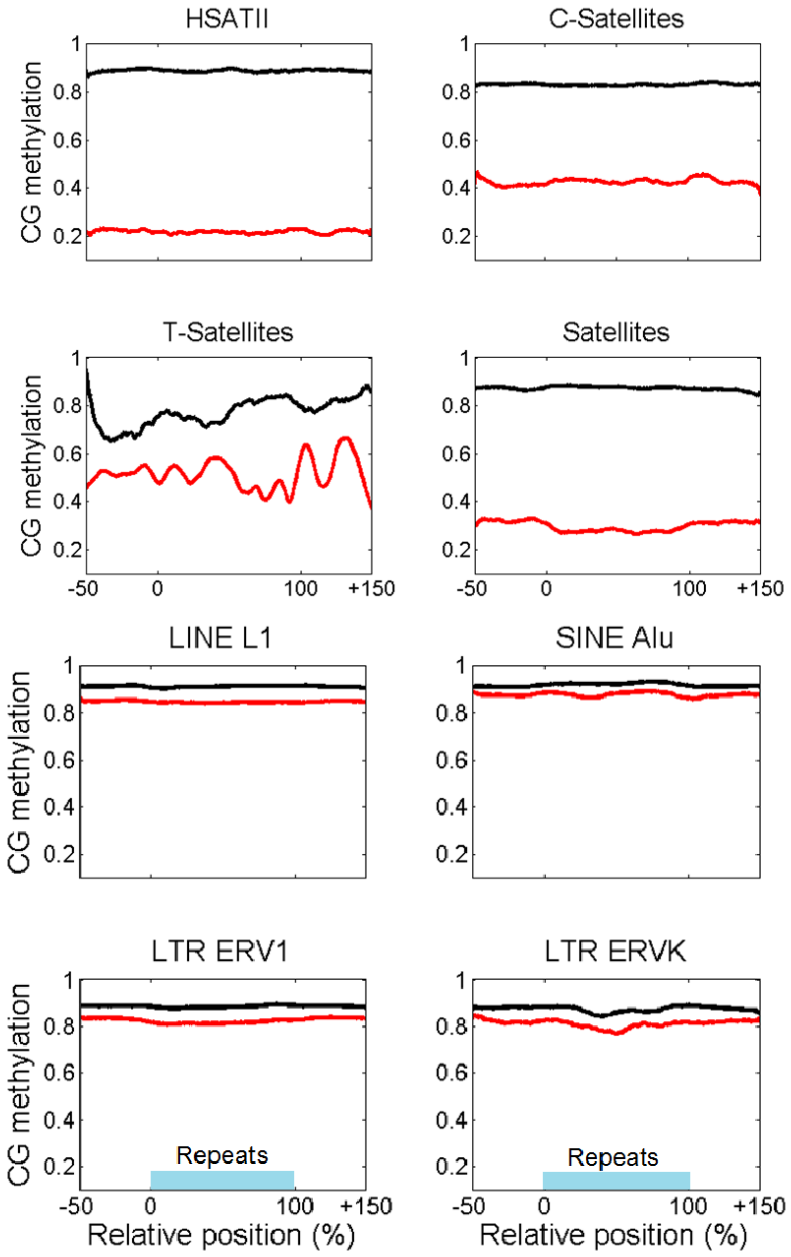

Figure S6. CG demethylation at repeats in ICF iPSCs are selective for satellite repeats. Metaplots across different classes of repeats. Positions are normalized by repeat length. C-satellites = centromere-satellites; T-satellites = telomeric satellites; HSATII = human satellite repeat 2; and "Satellites" includes all satellite-type repeats. Black: control iPSCs (IMR90iPS, FF1911iPS); Red: ICF1-1 and -2 iPSCs

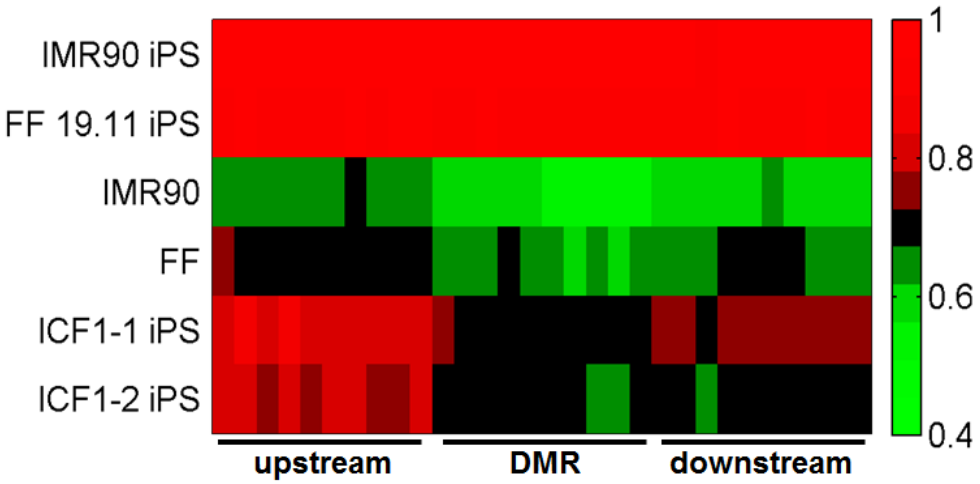

Fig. S7. Megabase domains of demethylation. Heatmap of average methylation levels at regions of hypomethylation identified in ICF1 iPSCs. For reference, fibroblast cells from control iPSCs are shown to show *de novo* methylation is impaired in ICF1 iPSCs.

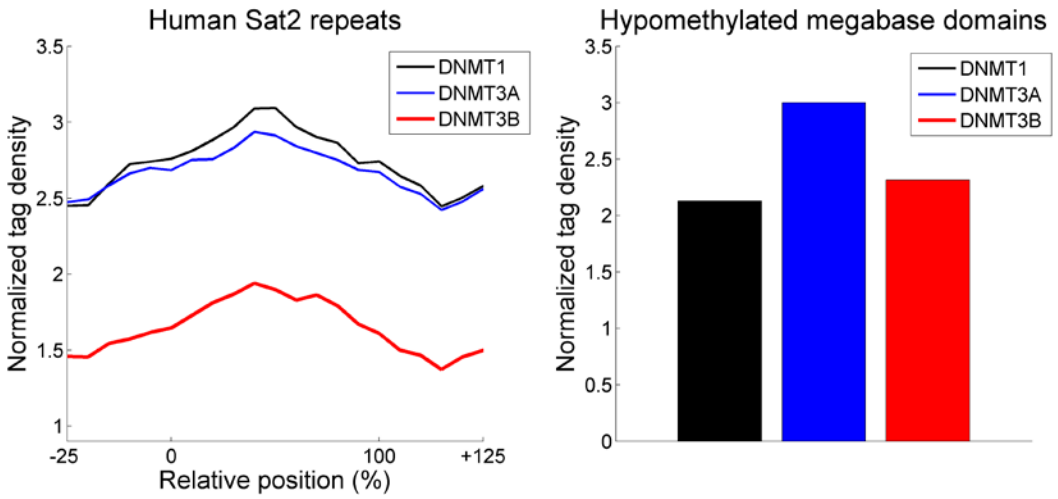

Fig. S8. Hypomethylated regions do not correlate with DNMT3B binding in pluripotent stem cells. A. Metaplot of normalized DNMT tag enrichment at human satellite 2 repeats which are known to be hypomethylated in ICF1 iPSCs. **B.** Normalized tag count of DNMT tags at regions of hypomethylation identified in ICF1 iPSCs (as shown in Fig. S7). DNMT ChIP-seq binding data was re-mapped using public data from Jin et al. (2012, *Cell Reports*). Briefly, reads were mapped to the hg18 genome with Bowtie using default parameters. Only uniquely mapped reads were accepted and reads considered PCR duplicated were removed.

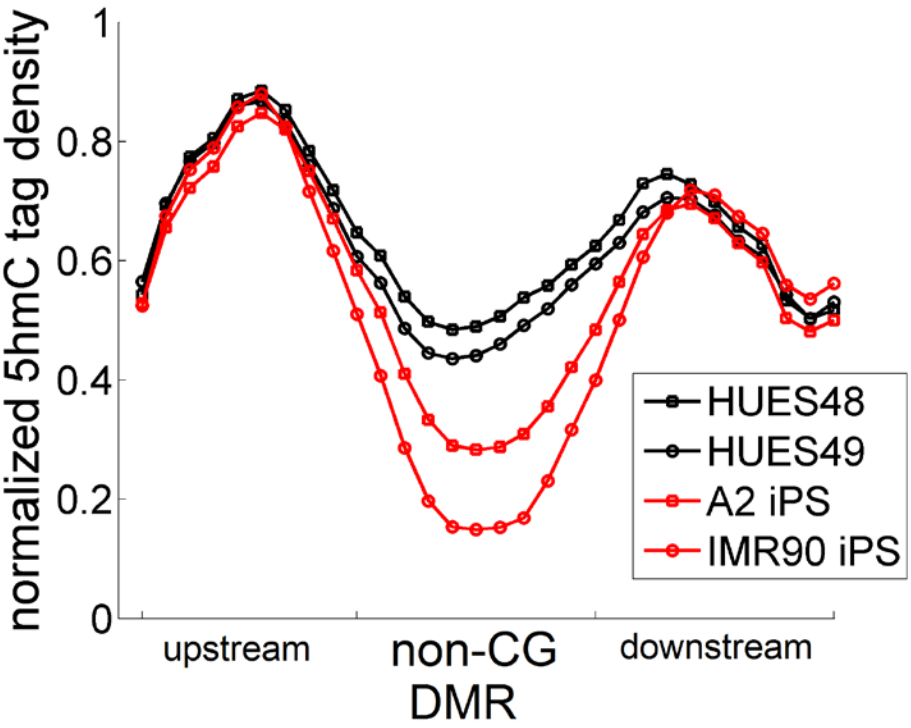

Fig. S9. Non-CG DMRs are flanked by high enrichment of 5hmC. Metaplot of 5hmC enrichment at non-CG DMRs as previously described by Lister et al. 5hmC ChIP-seq data was re-analyzed from Wang et al. 2013. *Nat Cell Biol.* Briefly, reads were mapped to the hg18 genome with Bowtie using default parameters. Only uniquely mapped reads were accepted and reads considered PCR duplicated were removed. Upstream and downstream regions were normalized based on half of the non-CG DMR length. 5hmC tag density was normalized by the maximum enrichment across the windows analyzed.

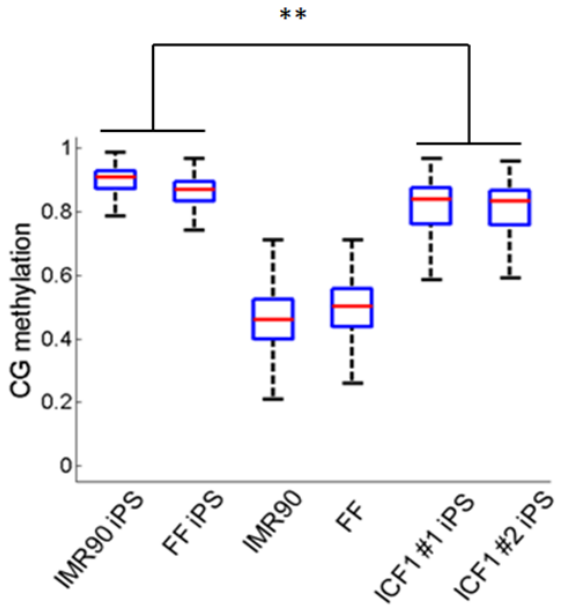

Fig. S10. Methylation status of partially methylated domains (PMDs). All PMD domains are as previously defined by Lister et al., (2011) and partitioned into 10kb windows. The distribution of average methylation of the 10kb windows are shown as boxplot (red line is median methylation of all windows). ** indicates significant distribution difference between control and ICF1 iPSCs (p<0.01, KS-test).

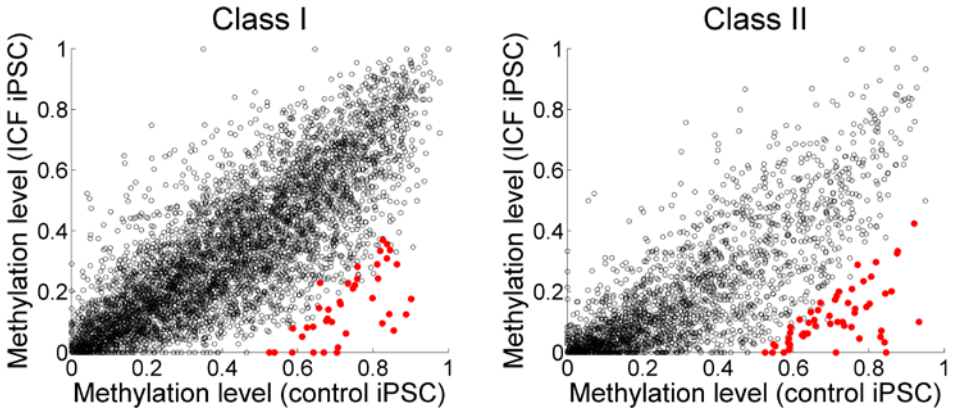

Fig. S11. Class I and Class II demethylation in ICF1 iPSCs. Class I and Class II enhancer regions are as previously defined by Rada-Iglesias et al. (2011). Average CG methylation of enhancers were plotted and significantly demethylated enhancers are colored in red (*delta-beta* > 50%, Benjamani-Hochberg adjusted FDR < 0.01).

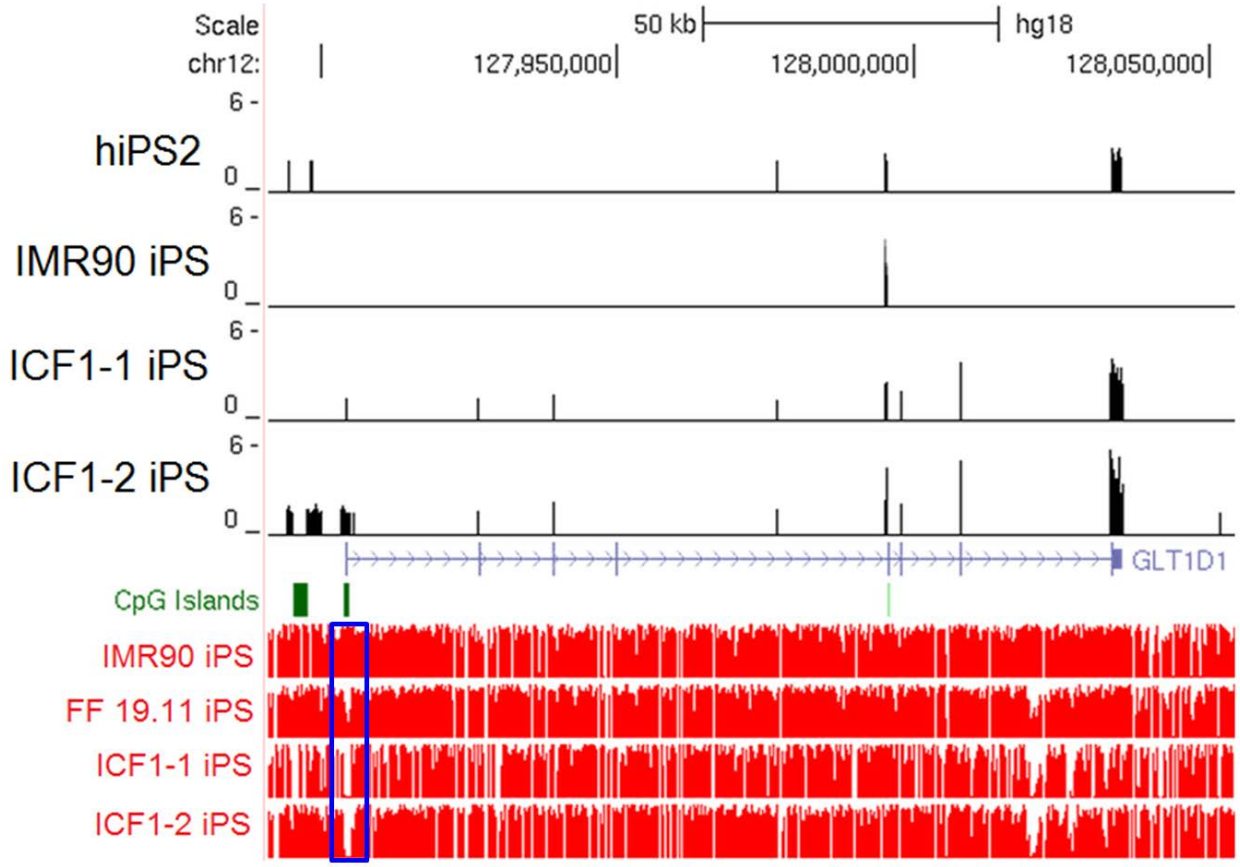

Fig. S12. Selective promoter demethylation example. Genome browser view of the *GLT1D1* gene locus. Top four tracks (in black) are normalized RNA-seq reads (RPM) and bottom four tracks are CG methylation levels (in red) as measured by bisulfite sequencing (between 0 and 1). Selective promoters hypomethylated is highlighted in blue bar.

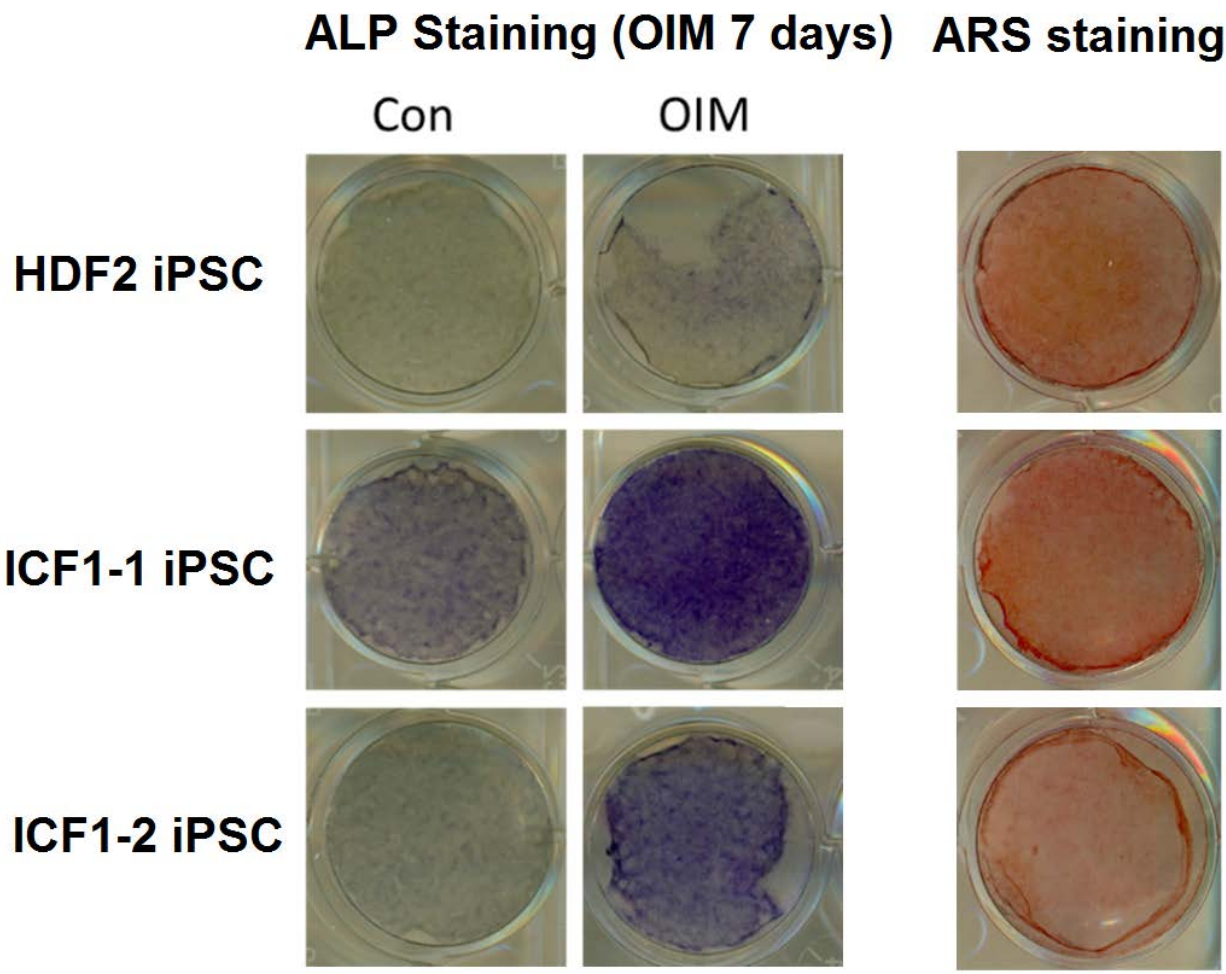

Fig. S13. MSC differentiation of control and ICF1 iPSCs. Human ESCs and iPSCs were cultured in bFGF-depleted hESCs for 7 days and directed to form embryoid bodies. MSCs were collected by flow cytometry using antibodies are CD73 and CD146 (see Material/Methods). MSCs were grown in media containing 100μM/ml ascorbic acid, 2mM β-glycerophosphate, and 10nM dexamethasone to induce mineralization as previously described (Ye et al., 2012. *Cell Stem Cell*). Alkaline phosphatase (ALP) activity and Alizarin Red staining (ARS) was performed as previously described (Chang et al., 2009. *Nat. Med.*). While ALP staining is commonly used for marking pluripotent stem cells, it is also a useful mark for staining osteogenic cells which expresses high levels of alkaline phosphatase (a key enzyme for producing the phosphate substrates needed for mineral deposition and calcification in osteoblasts). OIM: osteo-induction medium.

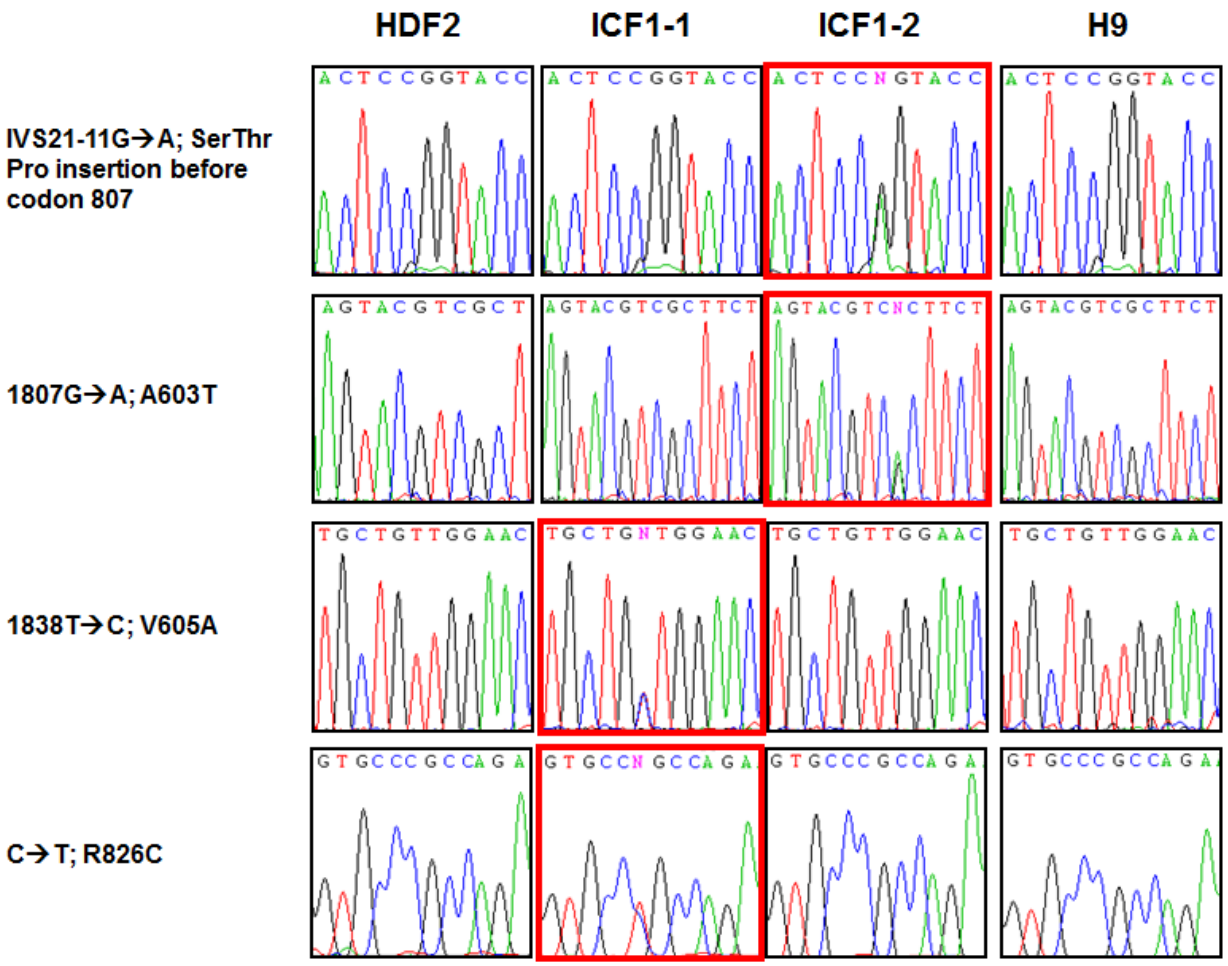

Fig. S14. DNMT3B mutations confirmation via Sanger sequencing.